Natural Resources Canada | Ressources naturelles Canada

GEOLOGICAL SURVEY OF CANADA
OPEN FILE 8880

U-Pb geochronological results from the Nonacho Lake area (NTS 75-F), Northwest Territories

D. Regis, R. Canam, and E. Martel

2022

Canada

GEOLOGICAL SURVEY OF CANADA
OPEN FILE 8880

U-Pb geochronological results from the Nonacho Lake area (NTS 75-F), Northwest Territories

D. Regis[1], R. Canam[2], and E. Martel[2]

[1]Geological Survey of Canada, 601 Booth Street, Ottawa, Ontario
[2]Northwest Territories Geological Survey, 4601 52nd Avenue, Yellowknife, Northwest Territories

2022

Permanent link: https://doi.org/10.4095/329884

This publication is available for free download through GEOSCAN (https://geoscan.nrcan.gc.ca/).

Recommended citation
Regis, D., Canam, R., and Martel, E., 2022. U-Pb geochronological results from the Nonacho Lake area (NTS 75-F), Northwest Territories; Geological Survey of Canada, Open File 8880, 1 .zip file. https://doi.org/10.4095/329884

Publications in this series have not been edited; they are released as submitted by the author.

Introduction

This Open File presents new SHRIMP (Sensitive High-Resolution Ion Microprobe) U–Pb zircon geochronological results for fifteen plutonic samples from the Nonacho Lake area (NTS 75F) along the western margin of the Rae craton (Northwest Territories). Detailed mapping and sampling for U–Pb geochronology was carried out by Northwest Territories Geological Survey (NTGS) and academic partners as part of the 'Nonacho Bedrock NTGS Mapping Project' during the 2018-2020 field seasons. Samples have been collected from the Nonacho basement to unravel key age relationships between units, place time constraints on the geologic evolution of the southwestern Rae margin, and assess its mineral potential. The locations of samples are shown in Figure 2 and a summary of age results is presented in Table 1. Sample information and the presentation and interpretation of the U-Pb data are provided for each sample in the following sections. The U-Pb analytical data are presented in Appendix 1.

Geological background

The study area (NTS 75F, Nonacho Lake) is located in the westernmost region of the South Rae craton, in the southeastern Northwest Territories (Fig. 1). This region is situated to the east of the Taltson magmatic zone and basement complex (Bostock, 2014) and within the Porter domain identified in the GEM-2 South Rae project (Davis et al., 2015; Martel et al., 2020). However, the boundary between the Taltson basement complex and the Nonacho basement complex is still ambiguous, and the western extent of the Porter domain has not yet been recognized.

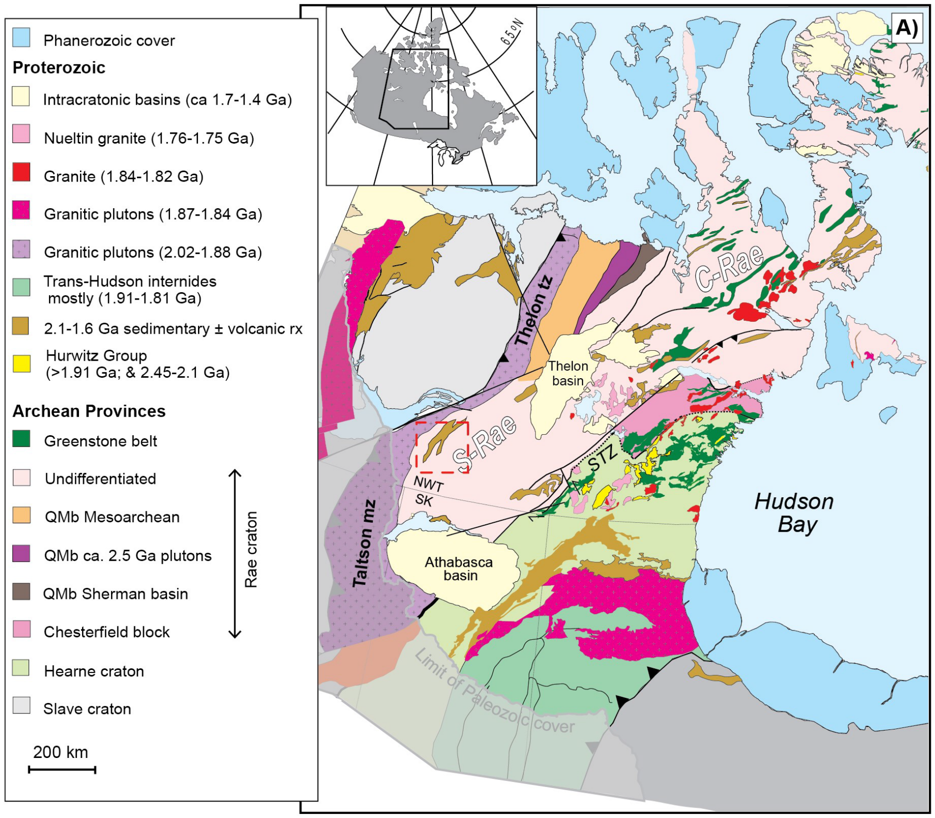

Figure 1: Regional tectonic domain map of NW Laurentia. The area of Figure 2 is shown by the red dashed rectangle. S-Rae: south Rae; C-Rae: central Rae; STZ: Snowbird Tectonic Zone; mz: magmatic zone; tz: tectonic zone.

The Nonacho Lake map sheet (Fig. 2) is composed of the Paleoproterozoic Nonacho Group unconformably overlying Archean to Paleoproterozoic granitic and gneissic basement rocks (Henderson, 1939; Taylor, 1971). The Nonacho Group is a succession of 1.91-1.83 Ga unmetamorphosed to sub-greenschist facies siliciclastic rocks interpreted to have been deposited in an alluvial, fluvial, and lacustrine environment (Aspler, 1985; Bostock and van Breemen, 1992; van Breemen et al., 2013). A recent reappraisal of the basin provides evidence for marine incursion during the deposition of the Nonacho Group (Ielpi et al., 2021).

The basement rocks are generally thought to be Archean and remain mostly undivided granitoid and granitic gneiss (Henderson, 1939; McGlynn, 1966). Sporadic exposures of quartzite, greywacke, amphibolite, hornblende gneiss, and paragneiss were identified in this map sheet and interpreted as possible remnants of supracrustal belts older than the surrounding granitoids (Henderson, 1939). While multiple tectonometamorphic events have been recognized along the western margin of the Rae craton including the 2.5-2.28 Ga Arrowsmith Orogeny (Berman et al., 2013; Schultz et al., 2007), the 2.0-1.91 Ga Taltson Orogeny (Berman and Bostock, 1997; Bostock and Loveridge, 1988), and the 1.9-1.8 Ga Trans-Hudson Orogenies (Corrigan et al., 2009), the exact influence of each of these events on the Nonacho Lake area is unknown due to a lack of data. The limited isotopic data available for the basement rocks yield hornblende $^{40}Ar/^{39}Ar$ dates of ca. 2240 Ma (Burwash and Baadsgaard, 1962), and mica $^{40}Ar/^{39}Ar$ dates of ca. 1800 Ma (Lowdon et al., 1963; Wanless et al., 1968). Henderson interpreted these ages to mostly reflect the presence of Archean volcanic, sedimentary and magmatic rocks later intruded and/or affected by the Hudsonian orogeny.

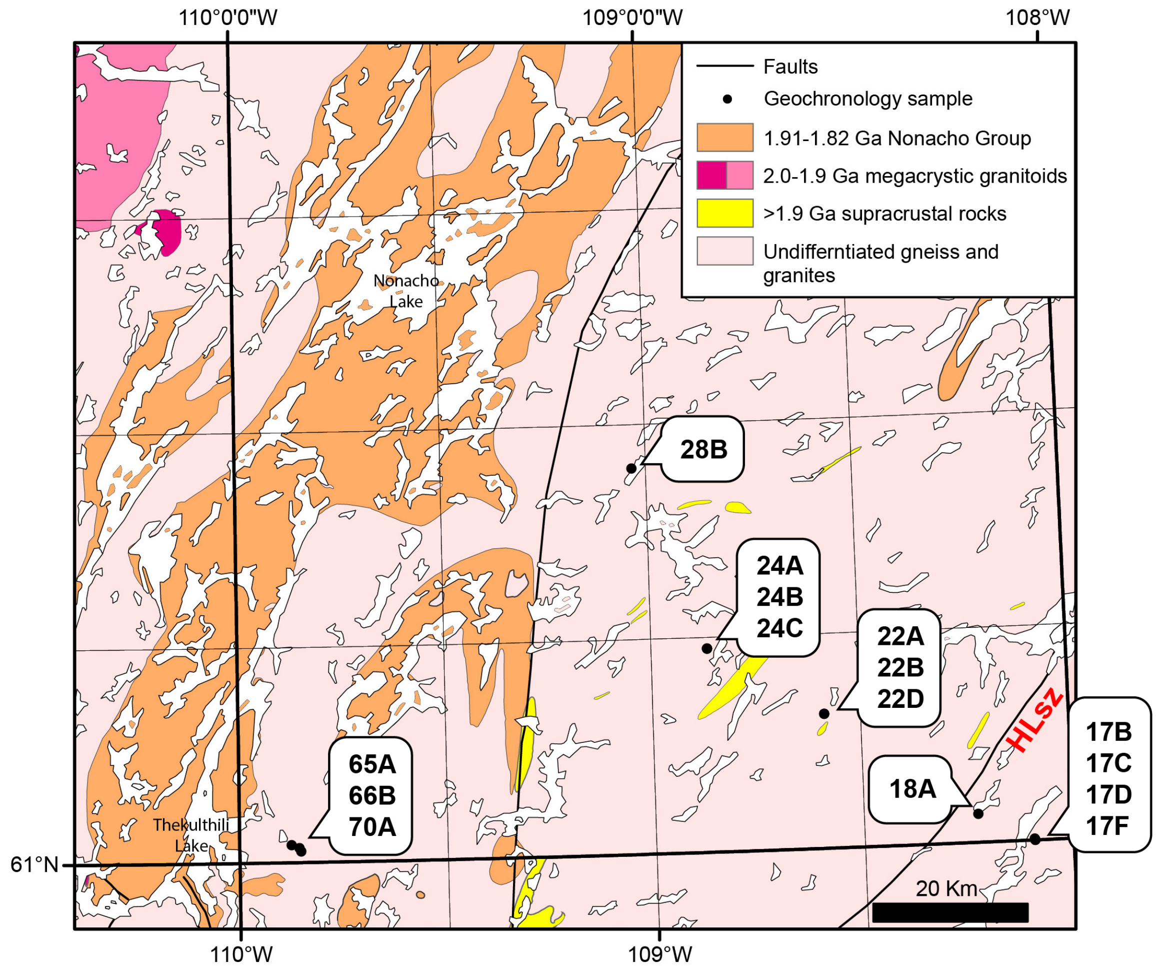

Figure 2: Simplified, preliminary geological map of the Nonacho Lake area (modified from Pehrsson 2014) showing the locations of zircon geochronology samples described in the text (black circles and labels). HLsz: Howard Lake shear zone.

Renewed bedrock mapping of the Nonacho Lake sheet was conducted by the NTGS during the 2019 and 2020 field seasons, following reconnaissance mapping in 2018 and building on the previous mapping by Henderson (1939) and Taylor (1971). This mapping identified five new lithotectonic domains (Martel et al., in prep). The geochronological results from this report will be incorporated with the new bedrock mapping to refine the domains of the Nonacho Lake map sheet.

Summary of Results

Sample number	*Lab Z number*	*Metamorphism*	*Crystallization*	*Inheritance*
20EM17B	12646	2572.9±3.5 Ma	2587.9±2.4 Ma	
20EM17C	12645		2586.1±1.8 Ma	
20EM17D	12681	~2575 Ma	2592.6±2.3 Ma	
20EM17F	12644		2585.5±2.3 Ma	
20EM18A	12643		2566.2±1.3 Ma	2608-2578 Ma
20EM22A	12642		2580.3±1.6 Ma	
20EM22B	12658		2582.3±1.4 Ma	
20EM22D	12659		2581.8±1.8 Ma	
20EM24A	12660		2578.2±1.9 Ma	
20EM24B	12661		2585.9±2.4 Ma	
20EM24C	12662		2514±21 Ma	2595-2559 Ma
20EM28B	12682	2423.4±3.8 Ma 2393.9±3.0 Ma	2518.1±5.1 Ma	
20EM65A	12683	2445-2389 Ma	2516.0±3.1 Ma	
20EM66B	12684		2578.5±3.8 Ma	
20EM70A	12685	2414-2379 Ma	2515.7±3.9 Ma	2653-2559 Ma

Table 1: Summary of the SHRIMP U-Pb zircon geochronology results for the Nonacho Lake area.

Analytical Methods

Samples were processed using standard crushing, grinding, Wilfley table, magnetic (Frantz™ isodynamic separator), and heavy-liquid separation techniques at the Geological Survey of Canada (GSC, Ottawa). Zircon crystals were hand-picked for quality and morphological variety (~120 grains per sample) and then mounted in 2.5 cm diameter epoxy pucks with fragments of standard reference materials Z-6266 (primary standard, $^{206}Pb/^{238}U$ age = 559 Ma) and Z-1242 (secondary standard $^{207}Pb/^{206}Pb$ age = 2679.7 Ma). The mounts were polished to the midpoint using 9, 6, and 1 µm diamond compound to reveal internal features (zoning, alteration, cracks) using backscatter electron (BSE) and cathodoluminescence (CL) images acquired using a Tescan MIRA Field Emission Scanning Electron Microscope (FEG-SEM). U–Pb geochronology was performed using the SHRIMP housed in the J.C. Roddick Ion Microprobe facility at the GSC, Ottawa. SHRIMP analytical procedures were followed as per Stern (1997), and Stern and Amelin (2003). Fifteen samples were analyzed on three mounts in three separate analytical sessions (see Analytical Session Information). Analyses were conducted using an $^{16}O^-$ primary beam with a spot size of ~20 µm (depth ~1 µm). The data were collected in sets of six scans over 11 isotope masses of Zr, U, Pb, Th, Yb and Hf. A reference standard and secondary standard were generally analyzed every fifth analysis. Offline data processing was completed using SQUID2 (version 2.50.11.10.15, rev. 15 Oct 2011). Common lead correction utilized the Pb composition of the surface blank (Stern, 1997). Specific analytical details for each sample are given in the Analytical Session Information table at the beginning of the supplementary Excel U–Pb data table.

Isoplot v.4.15 (Ludwig, 2009) was used to generate concordia plots and to calculate regression ages and weighted ages. Error ellipses on the concordia plots and the weighted mean errors are reported in the text and figures at 95% confidence intervals (unless otherwise stated). MSWD: Mean Square Weighted Deviation, p.o.f.: probability of fit.

Analytical Session Information

IP	Kohler	Scans	Primary Standard	n (rej.)	1σ External Calibration Error (%)	Z-1242 Age (Ma)	Z-1242 Age Error (2SE)	n Z-1242 (rej.)	MSWD	Mass Frac. Value	Samples (Z#)				
990	100a	6	Z-6266	44 (0)	0.76	2678.2	2.6	35 (2)	1.4	1.0000	***12642***	***12643***	***12644***	***12645***	***12646***
996	100b	6	Z-6266	39 (0)	0.57	2681.7	2.2	34 (0)	0.8	1.0000	***12658***	***12659***	***12660***	***12661***	***12662***
998	70a	6	Z-6266	47 (3)	0.77	2677.9	3.5	43 (0)	1.2	1.0000	***12681***	***12682***	***12683***	***12684***	***12685***

RESULTS

1. Sample 20EM17B

This sample is located south of the Howard Lake shear zone (HLsz, Fig. 2) from a well exposed, complex outcrop displaying several rock types and contact relationships. Sample *20EM17B* is a light pink, medium-grained, weakly magnetic, foliated, hornblende monzonite (Fig. 3). The monzonite has a gradual contact with an amphibolite unit and is cross-cut by the quartz-ribbon granite (*20EM17F*). Xenoliths of the hornblende monzonite are observed in the andesite samples (*20EM17C*, *20EM17D*).

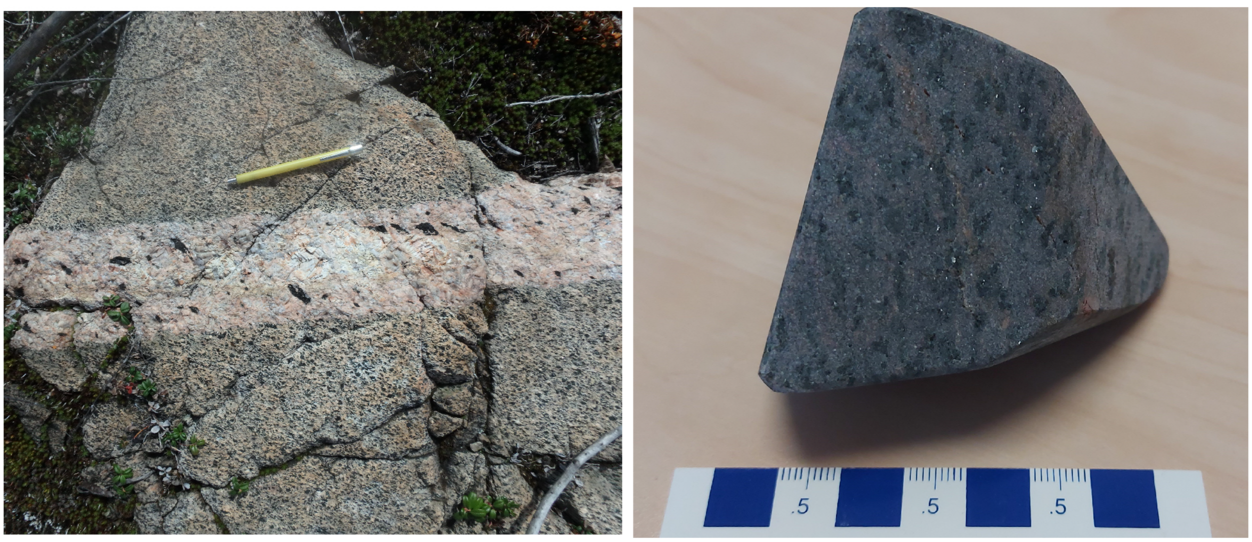

Figure 3: Field photograph of foliated, hornblende monzonite (20EM17B) crosscut by a late granitic dyke (left) and photograph of the sample processed for U-Pb geochronology (right). Courtesy of Edith Martel.

20EM17B: Zircon description

Zircon crystals recovered from sample *20EM17B* occur as pale to dark brown, variably fractured, euhedral to subhedral prisms (100-350 µm, Fig. 4a). Cathodoluminescence (CL) images reveal distinct zones: dark zircon portions with faint oscillatory zoning (grain #12, Fig. 4c) are locally overgrown by CL-dark homogeneous rims (grain # 43, Fig. 4d). Two grains preserve anhedral embayed bright cores characterized by oscillatory growth zoning (Fig. 4c). Some crystals have thin (<5µm) bright external rims (grain #12, Fig. 4c). No analyses were performed on these external rims due to their small size.

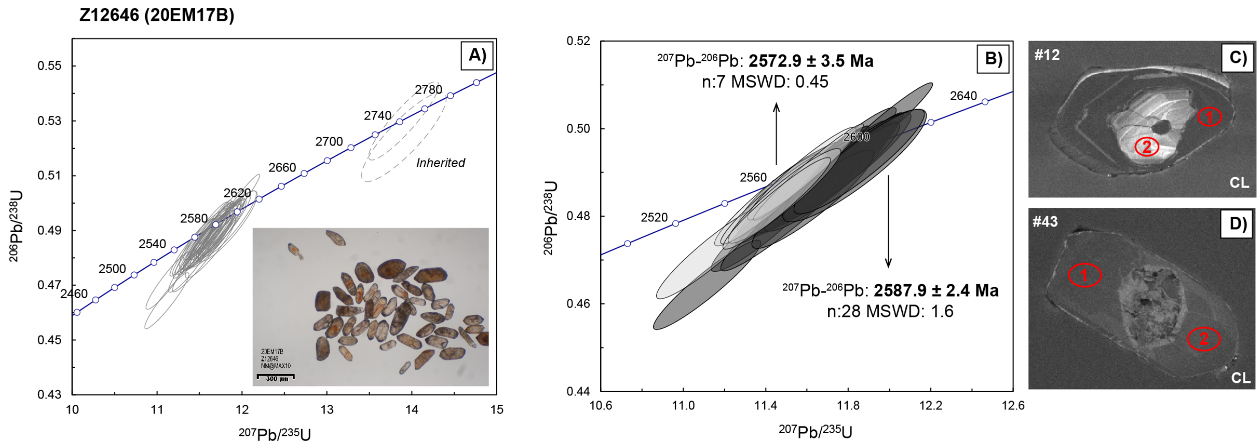

Figure 4: (a, b) Concordia diagram showing U-Pb SHRIMP results. (b) Dark grey ellipses indicate the analyses used for the crystallization age calculation. Light grey ellipses indicate the analyses used for the CL-dark rim age calculation. Error ellipses are at 95% confidence level. (c, d) CL images of grains #12 and #43 and spot locations (the red ellipse is ~20µm). The number in the ellipses corresponds to the analysis number (Appendix 1).

20EM17B: U-Pb results and interpretation

Thirty-eight analyses on twenty-eight grains return ages ranging between 2.76 and 2.57 Ga (Fig. 4a, b, Appendix 1). Uranium contents range from 55 to 958 ppm. The two oldest analyses (2763 and 2744 Ma) were acquired on the two bright oscillatory-zoned cores (e.g., analysis #12.2, Fig. 4a, c), are distinctly older than the other analyses, and are interpreted as inherited. Twenty-eight analyses on the dark, oscillatory-zoned domains (e.g., analysis #12.1, Fig. 4b, c) define a single population with a weighted mean $^{207}Pb/^{206}Pb$ age of 2587.9 ± 2.4 (n = 28, MSWD = 1.6, Fig. 4b). This age is interpreted as the crystallization age of monzonite. Seven analyses on dark and homogeneous rims yield a weighted mean $^{207}Pb/^{206}Pb$ age of 2572.9 ± 3.5 (n = 7, MSWD = 0.45, Fig. 4b). We interpret this age as the time of a Neoarchean metamorphic recrystallization event or new growth stage.

2. <u>Sample 20EM17C</u>

Sample *20EM17C* is a greenish-grey, non-magnetic, foliated, feldspar-phyric andesite (Fig. 5). The andesite forms 5-10m thick bands and is associated with volcaniclastic layers. This sample is in contact with the amphibolite and hornblende monzonite units and is cross-cut by quartz-ribbon granite (*20EM17F*) and by leucogranite.

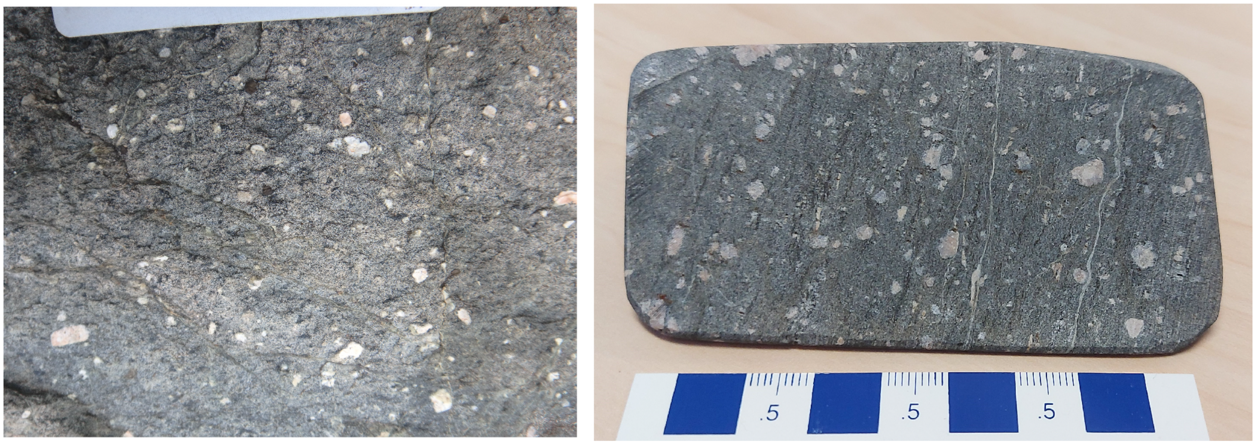

Figure 5: Field photograph of the foliated, feldspar-phyric andesite (20EM17C, left) and photograph of the sample processed for U-Pb geochronology (right). Courtesy of Edith Martel.

20EM17C: Zircon description

Zircon in sample *20EM17C* occur as pale to dark brown crystals. Most grains are prismatic and well-faceted with sizes ranging from 100 to 250 µm (Fig. 6a). All grains show a well-developed oscillatory zoning in CL images (Fig. 6b).

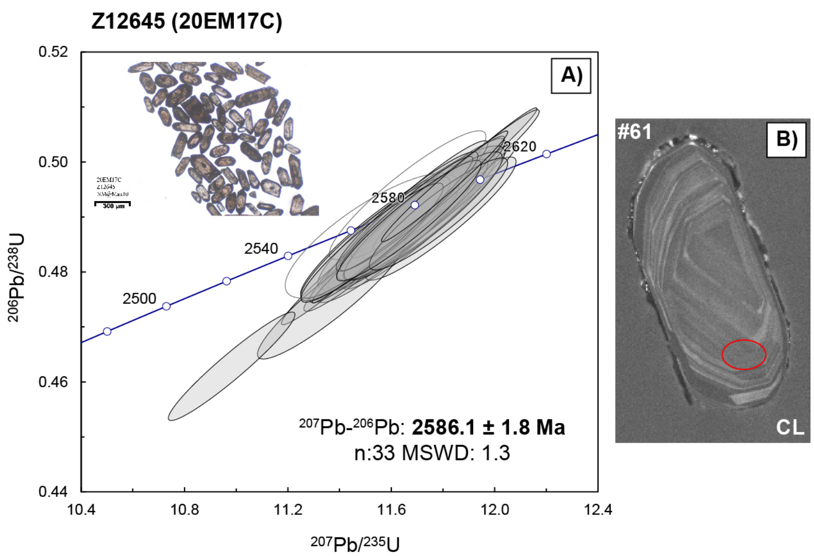

Figure 6: (a) Concordia diagram showing U-Pb SHRIMP results; grey ellipses indicate the analyses used for the age calculation. Error ellipses are at 95% confidence level. Inset: Plain light photomicrograph of zircon mounted for SHRIMP analysis. (b) CL image of grain #61 and a spot location (the red ellipse is ~20µm).

20EM17C: U-Pb results and interpretation

Thirty-five analyses were carried out on twenty-seven grains. Thirty-three analyses of oscillatory-zoned grains yield a weighted mean $^{207}Pb/^{206}Pb$ age of 2586.1 ± 1.8 Ma (MSWD = 1.3, Fig. 6a). Two slightly younger analyses have been excluded from the calculation assuming minor Pb-loss. This age is interpreted as the best estimate for the crystallization age of the rock.

3. Sample 20EM17D

Sample *20EM17D* is a greenish-grey, non-magnetic, foliated, aphanitic to feldspar-phyric andesite (Fig. 7). The andesite forms 5-10 m thick bands and is associated with volcaniclastic layers. This sample was collected approximately 20 m away from sample *20EM17C*.

Figure 7: Field photograph of the feldspar-phyric andesite (20EM17D, left) and photograph of the sample processed for U-Pb geochronology (right). Courtesy of Edith Martel.

20EM17D: Zircon description

Only 48 grains were recovered from sample *20EM17D.* Zircon crystals are light to pale brown in color with sizes ranging from 50 to 300 µm. Crystals are euhedral to subhedral with some rounding of terminations. In CL images all the zircon grains show distinct bright oscillatory zoning. Some grains are characterized by thin (<10 µm), highly fractured, dark, and homogenous rims overgrowing the oscillatory-zoned domains (grain #22, Fig. 8b). One crystal exhibited a rim large enough (ca. 60 µm) that allowed analysis by SHRIMP (grain #42, Fig. 8c).

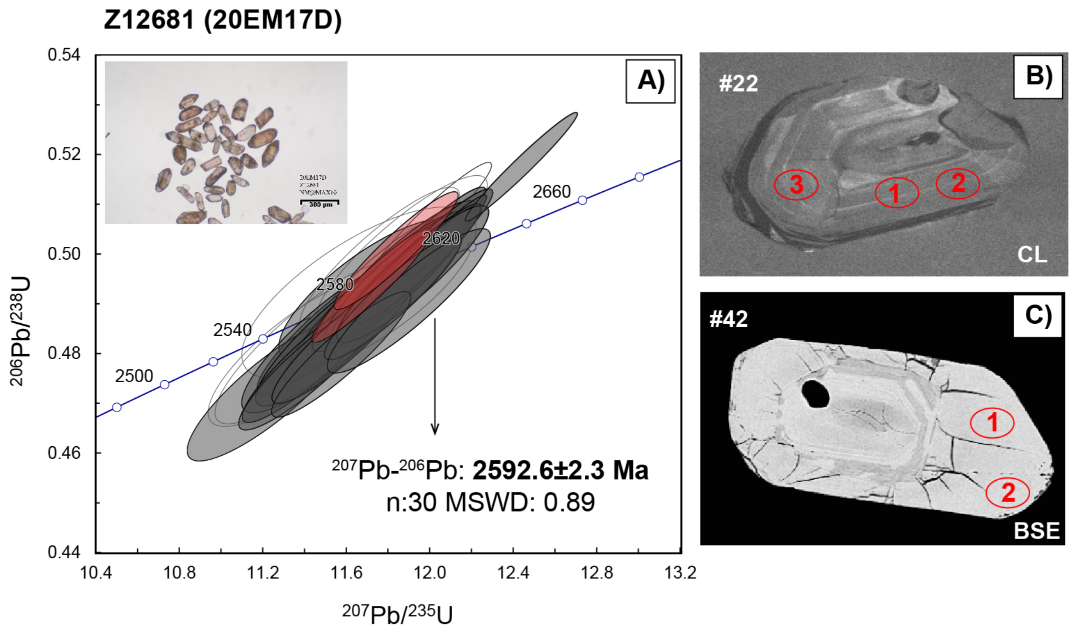

Figure 8: (a) Concordia diagram showing U-Pb SHRIMP results; grey ellipses indicate the analyses used for the age calculation. Red ellipses are analyses interpreted to reflect a metamorphic recrystallization stage. Error ellipses are at 95% confidence level. Inset: Plain light photomicrograph of zircon mounted for SHRIMP analysis. (b) CL image of grain #22 and spot locations. (c) Backscattered (BSE) image of grain #42 and spot locations (red ellipses are ~20µm).

20EM17D: U-Pb results and interpretation

Thirty-nine analyses were carried out on thirty grains. The oldest thirty analyses of oscillatory-zoned cores yield a weighted mean $^{207}Pb/^{206}Pb$ age of 2592.6 ± 2.3 Ma (MSWD = 0.89, Fig. 8a). The younger analyses are interpreted to reflect variable Pb-loss. Cores are characterized by Yb concentrations between 90 and 541 ppm. The recrystallized rims (grain #42) show different chemistry with lower Yb (ca. 60 ppm). The two analyses of the recrystallization domain (grain #42, Fig. 8c) return $^{207}Pb/^{206}Pb$ dates of 2572 ± 6 Ma and 2579 ± 5 Ma (1σ errors, Fig. 8a). The age of the oscillatory-zoned cores is interpreted as the crystallization age of the andesite. This age is slightly older than that of sample *20EM17C*, suggesting that the ca. 2586 Ma age of sample *20EM17C* represents a minimum crystallization age of the andesite. The dates obtained on the rim of grain #42 overlap within error of the age of the rims in sample *20EM17B*. Based on chemistry and textures, we interpret these dates to reflect a Neoarchean metamorphic recrystallization stage.

4. Sample 20EM17F

Sample *20EM17F* is a white to pink, leucocratic, medium- to coarse-grained, non-magnetic, feldspar-phenocrystic biotite-monzogranite (Fig. 9a). This sample is strongly foliated to mylonitic with quartz ribbons defining the foliation. The monzogranite intrudes the andesite samples (*20EM17C, D*, Fig. 9b) and the hornblende monzonite (*20EM17B*).

Figure 9: (a) Field photograph of the feldspar-phenocrystic biotite-monzogranite (20EM17F). (b) Field expression of the intrusive relationship between the monzogranite (20EM17F) and the andesite (20EM17C, D). Both units are crosscut by late thin granitic veins. Courtesy of Edith Martel.

20EM17F: Zircon description

Zircon crystals recovered are generally light to dark brown in colour with sizes ranging from 50 to 250 µm (Fig. 10). Crystals are euhedral to subhedral in shape with abundant fractures. Oscillatory zoning accentuated by secondary alteration is observed in CL images (Fig. 10b, c). No rims were observed.

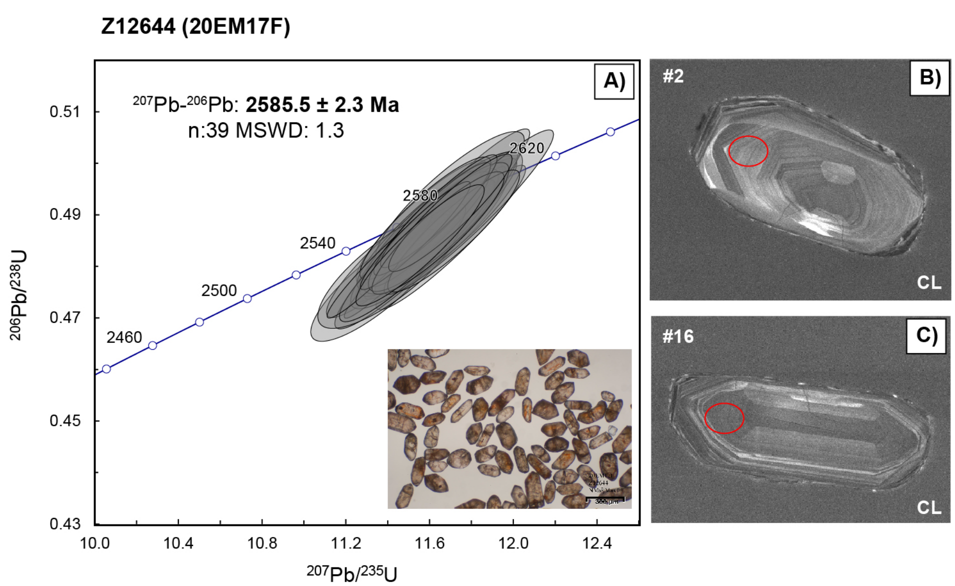

Figure 10: (a) Concordia diagram showing U-Pb SHRIMP results; grey ellipses indicate the analyses used for the age calculation. Error ellipses are at 95% confidence level. Inset: Plain light photomicrograph of zircon mounted for SHRIMP analysis. (b, c) CL images of grains #22 and #16 and spot locations; (red ellipses are ~20µm).

20EM17F: U-Pb results and interpretation

Thirty-nine analyses of oscillatory-zoned grains define a single age population with a weighted mean $^{207}Pb/^{206}Pb$ age of 2585.5 ± 2.3 Ma (MSWD = 1.3, Fig. 10a). This is interpreted as the crystallization age of the granite.

5. <u>Sample 20EM18A</u>

This sample is located immediately south of the Howard Lake shear zone (Fig. 2). *20EM18A* is a white to grey, leucocratic, medium-grained biotite-monzogranite with mm-sized pink garnet (Fig. 11). The monzogranite is strongly foliated. Contact relationships with other lithologies were not observed.

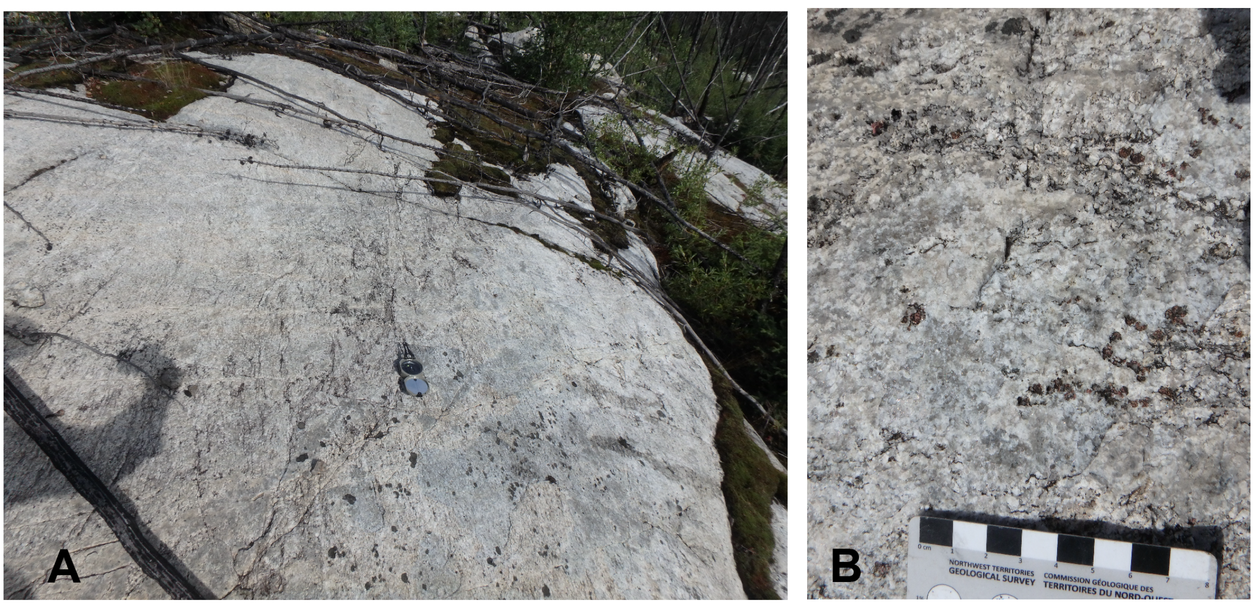

Figure 11: (a) Field photograph of the garnet-biotite monzogranite (20EM18A). (b) Detailed view of sample 20EM18A displaying mm-sized garnets in the monzogranite. Courtesy of Edith Martel.

20EM18A: Zircon description

Zircon occurs as large (100-400 µm) euhedral to subhedral, dark brown, and highly fractured prismatic crystals (Fig. 12a). Internal textures are characterized by oscillatory-zoned cores and darker homogeneous rims (Fig. 12d). Some of the rims have metamict interfaces that mimic faint oscillatory zoning.

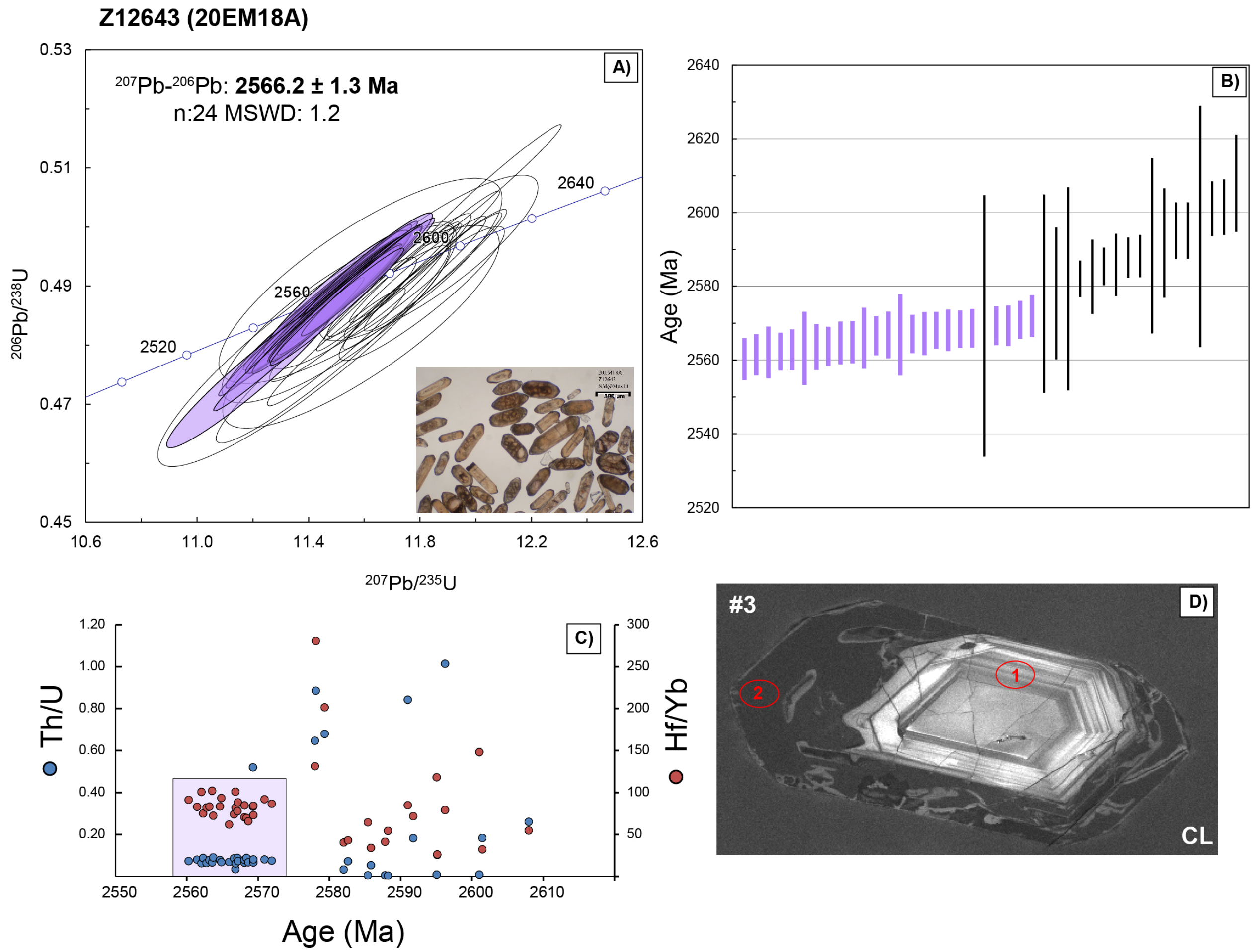

Figure 12: a) Concordia diagram showing U-Pb SHRIMP results; purple ellipses indicate the analyses used for the age calculation. Error ellipses are at 95% confidence level. Inset: plain light photomicrograph of zircon mounted for SHRIMP analysis. (b) Weighted average age plot; purple bars correspond to the purple ellipses in Fig. 12a. Dark bars correspond to core analyses that do not define a single age population. (c) Age (Ma) vs Th/U (axis on the left) and Hf/Yb (axis on the right) plot; analyses in the purple box correspond to the analyses used for age calculation. (d) CL image of grain #3 and spot locations (red ellipses are ~20µm).

20EM18A: U-Pb results and interpretation

Forty-two analyses carried out on thirty-one grains targeting both cores and rims yield a range of concordant to near concordant ages between 2608 and 2560 Ma. Interpretation of the age of this rock is not straightforward. Oscillatory-zoned cores analyses (ranging in age between 2608 and 2578 Ma and not defining a single age population) are characterized by variable Th/U (0.01-1.01) and variable Hf/Yb (26-281) compositions (Fig. 12c). The large chemical variability could indicate that these crystals are inherited from the surrounding rocks. Analyses carried out on the oscillatory-zoned dark rims are more homogenous in composition (Th/U: 0.03-0.09; Hf/Yb: 74-102, Fig. 12c), are reproducible (e.g., grains #14, #37, #104), and define one population with a weighted mean $^{207}Pb/^{206}Pb$ age of 2566.2 ± 1.3 Ma (n: 24, MSWD = 1.2, Fig.12a). The low Th/U ratio could be interpreted as an indication of a metamorphic origin for these domains. However, in this case, the low values are the result of high U concentrations (U: 800-1400 ppm). If the rims were to be metamorphic, they should be co-crystallizing with the garnet. However, Yb values for the rims are relatively high (170-250 ppm) for zircon crystallizing in the presence of HREE-bearing phases (e.g., garnet). Therefore, based on i) the U and Yb concentrations, ii) morphology and iii) faint oscillatory zoning of some of these domains, we interpret the 2566 Ma age as the crystallization age of the monzogranite.

6. Sample 20EM22A

This sample is located in a magnetic high north of the Howard Lake shear zone (Fig. 2). *20EM22A* is a light pink, medium- to coarse-grained, foliated, magnetic, hornblende quartz diorite (Fig. 13). This unit commonly contains xenoliths of hornblende diorite (*20EM22D*), however, the intrusive relationship between the quartz diorite (*20EM22A*) and the monzogranite (*20EM22B*) is uncertain.

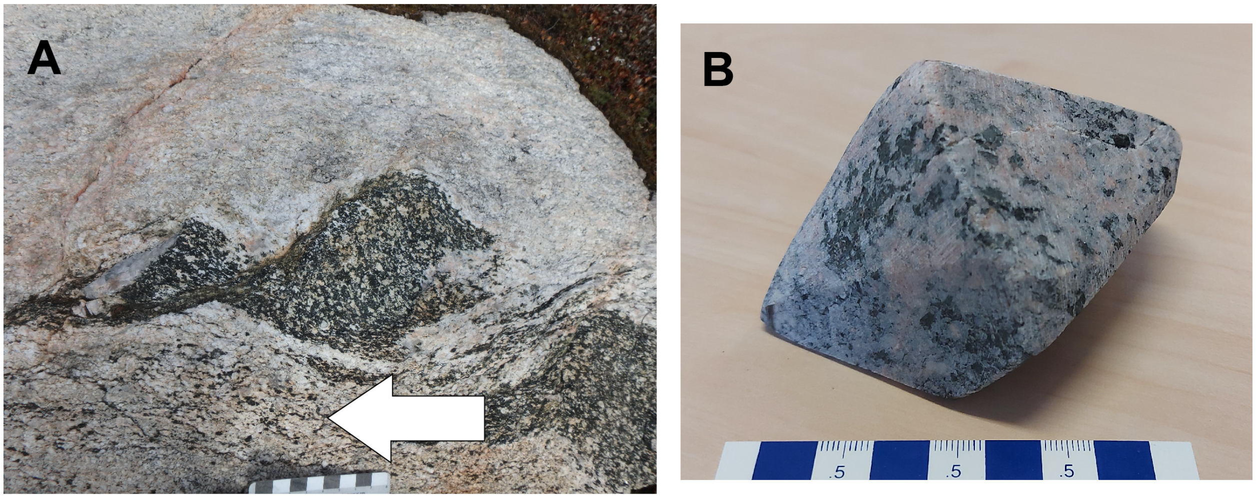

Figure 13: (a) Field photograph of the hornblende quartz diorite (20EM22A; indicated by the white arrow) illustrating the field relationship with the hornblende-biotite monzogranite (20EM22B, on top) and the diorite xenoliths (20EM22D). (b) Photograph of the sample processed for U-Pb geochronology. Courtesy of Edith Martel.

20EM22A: Zircon description

Zircon grains recovered from sample *20EM22A* are typically pale to dark brown (Fig. 14a). Crystals are generally multi-faceted elongated prisms. CL images reveal internal well-defined oscillatory growth zoning typical of igneous growth (Fig. 14b). No rims were observed.

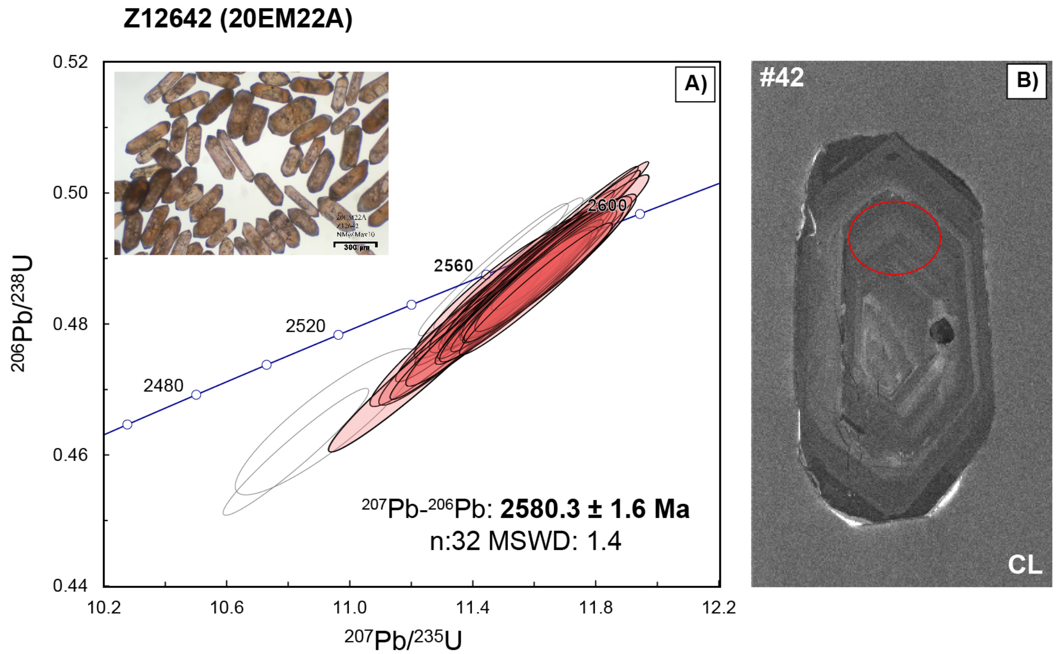

Figure 14: (a) Concordia diagram showing U-Pb SHRIMP results; red ellipses indicate the analyses used for the age calculation. Error ellipses are at 95% confidence level. Inset: Plain light photomicrograph of zircon mounted for SHRIMP analysis. (b) CL image of grain #42 and the spot location; (the red ellipse is ~20µm).

20EM22A: U-Pb results and interpretation

Thirty-seven zircon analyses on thirty grains yield a range of ages from 2591 to 2561 Ma (Fig. 14a). The thirty-two reproducible oldest analyses yield a weighted mean $^{207}Pb/^{206}Pb$ age of 2580.3 ± 1.6 (MSWD = 1.4, Fig.14a). This age is interpreted as the crystallization age of the granite. The younger analyses are interpreted to reflect variable Pb-loss from the Neoarchean crystallization age.

7. Sample 20EM22B

This sample is located in a magnetic high north of the Howard Lake shear zone (Fig. 2). *20EM22B* is white to pink, medium-to coarse-grained, hornblende-biotite monzogranite with rare feldspar megacrysts (Fig. 15). This sample is strongly foliated to mylonitic with quartz ribbons defining the foliation.

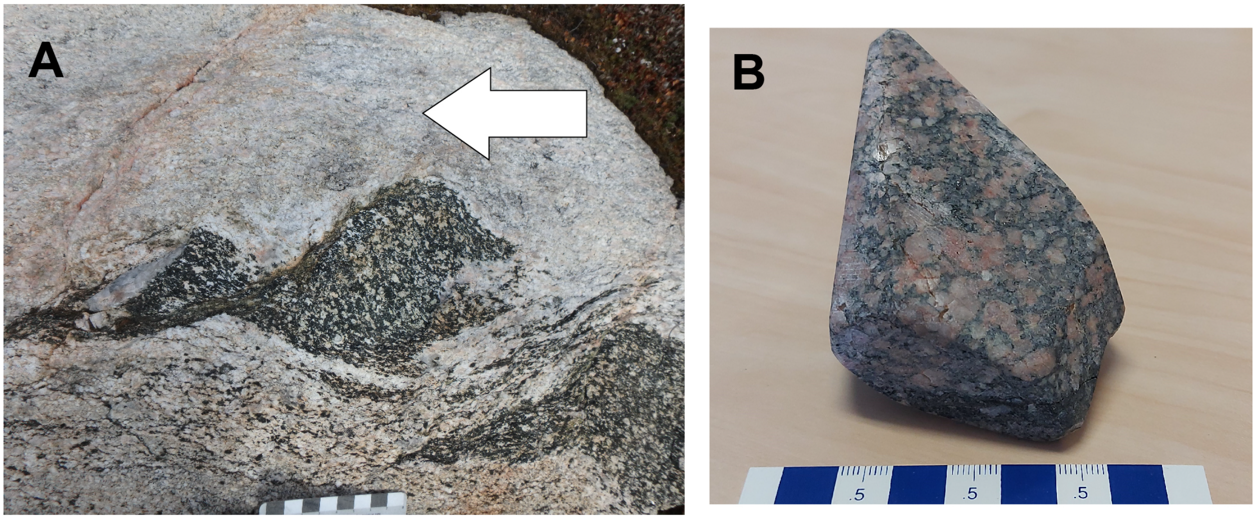

Figure 15: (a) Field photograph of the hornblende-biotite monzogranite (20EM22B; white arrow). (b) Photograph of the sample processed for U-Pb geochronology. Courtesy of Edith Martel.

20EM22B: Zircon description

Zircon occurs as medium to large (200-400 µm) subhedral, dark brown, and highly fractured prismatic crystals (Fig. 16a). Internal CL textures are characterized by oscillatory-zoned cores (Fig. 16b) and rare bright thin (<5µm) rims (Fig. 16c). No analyses were performed on the rims.

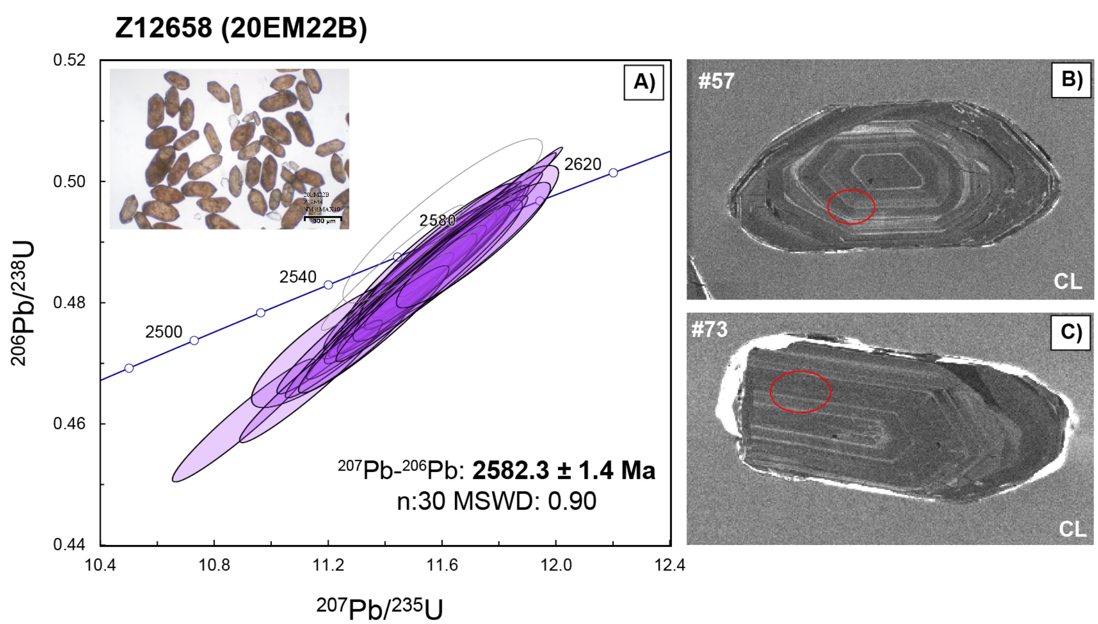

Figure 16: (a) Concordia diagram showing U-Pb SHRIMP results; purple ellipses indicate the analyses used for the age calculation. Error ellipses are at 95% confidence level. Inset: Plain light photomicrograph of zircon mounted for SHRIMP analysis. (b, c) CL images of grains #57 and #73 and spot locations; (red ellipses are ~20µm).

20EM22B: U-Pb results and interpretation

Thirty-two analyses of thirty-two oscillatory zoned zircon yield a weighted mean $^{207}Pb/^{206}Pb$ age of 2582.3 ± 1.4 Ma (MSWD = 0.90, Fig. 16a). This is interpreted as the crystallization age of the monzogranite. Some oscillatory zoned material have younger ages of ca. 2.56 Ga, which may indicate some Pb-loss. The crystallization age of the monzogranite overlaps within error with the age of sample *20EM22A*.

8. <u>Sample 20EM22D</u>

This sample is located in a magnetic high north of the Howard Lake shear zone (Fig. 2). *20EM22D* is a medium-grained, hornblende diorite, commonly found as dm- to cm-scale xenoliths (Fig. 17) within the hornblende quartz diorite (*20EM22A*) and the hornblende-biotite monzogranite (*20EM22B*). The diorite xenoliths display a foliation with a different orientation than that of the surrounding granitoids.

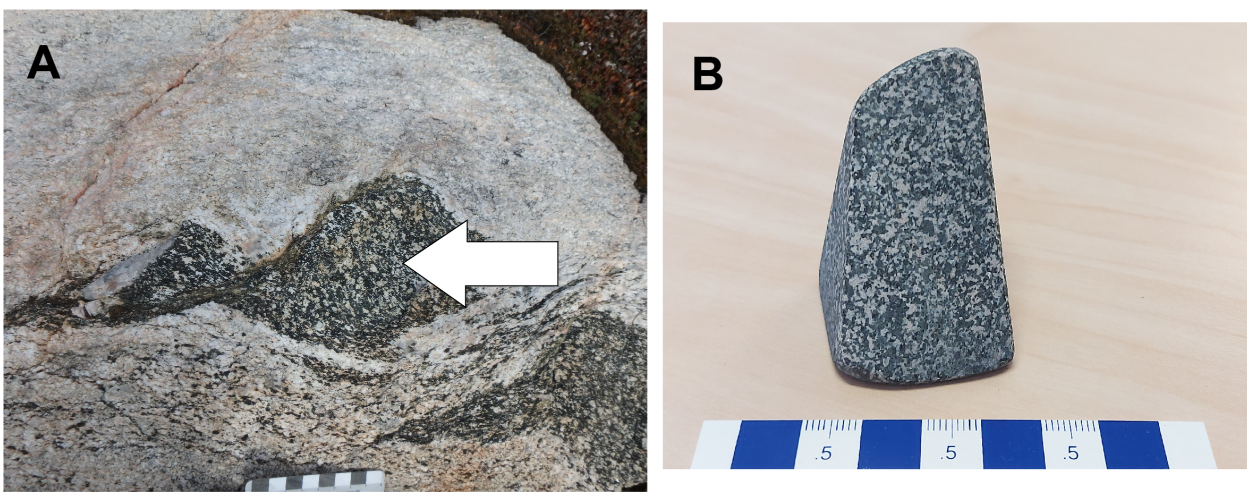

Figure 17: (a) Field photograph of the hornblende diorite xenoliths (20EM22D) within hornblende quartz diorite (20EM22A; top) and hornblende-biotite monzogranite (20EM22B; bottom). (b) Photograph of the sample processed for U-Pb geochronology. Courtesy of Edith Martel.

20EM22D: Zircon description

Zircon in sample *20EM22D* form subhedral to anhedral turbid and altered crystals (Fig. 18a). BSE images show high degrees of alteration. In some cases, a faint oscillatory zoning is accentuated by secondary alteration (Fig. 18b, c).

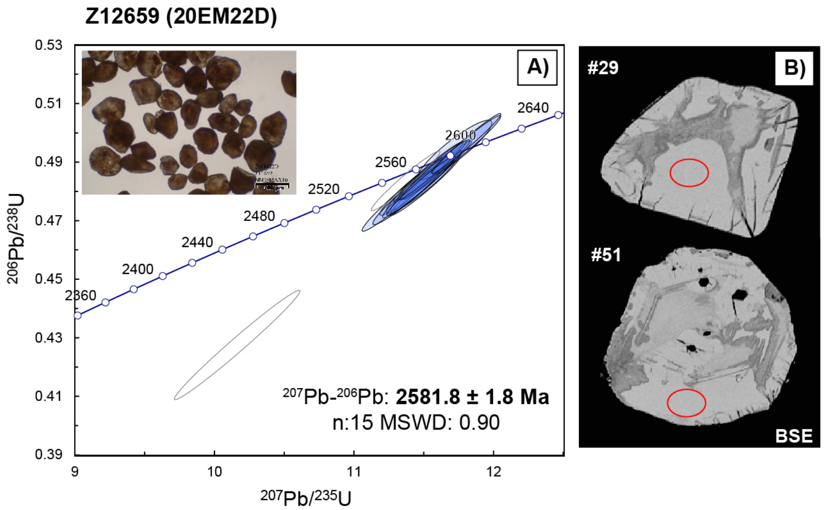

Figure 18: (a) Concordia diagram showing U-Pb SHRIMP results; blue ellipses indicate the analyses used for the age calculation. Error ellipses are at 95% confidence level. Inset: Plain light photomicrograph of zircon mounted for SHRIMP analysis. (b, c) BSE images of grains #29 and #51 and spot locations (red ellipses are ~20µm).

20EM22D: U-Pb results and interpretation

Due to the high degree of alteration, only a few grains were analyzed. A total of 17 analyses on 16 grains yield a weighted mean $^{207}Pb/^{206}Pb$ age of 2581.8 ± 1.8 Ma (MSWD = 0.9, Fig. 18a). Two analyses were excluded from the calculation.

9. Sample 20EM24A

Sample *20EM24A* is black and white, medium- to coarse-grained, foliated, hornblende monzogabbro. Monzogabbro occurs as m- to cm-scale xenoliths in xenolith-rich bands approximately fifteen meters wide (Fig. 19). The monzogabbro xenoliths are contained within quartz monzodiorite (*20EM24B*) and within biotite-monzogranite (*20EM24C*).

Figure 19: (a) Field photograph of monzogabbro xenoliths (20EM24A) contained within quartz monzodiorite (*20EM24B*). (b) Photograph of the sample processed for U-Pb geochronology. Courtesy of Edith Martel.

20EM24A: Zircon description

The zircon recovered from sample *20EM24A* are stubby to subhedral prismatic crystals (Fig. 20). The grains are generally of poor quality, moderately turbid, light to dark brown with some orange iron staining and show minor fracturing. Grain size ranges from 50 µm to 200 µm.

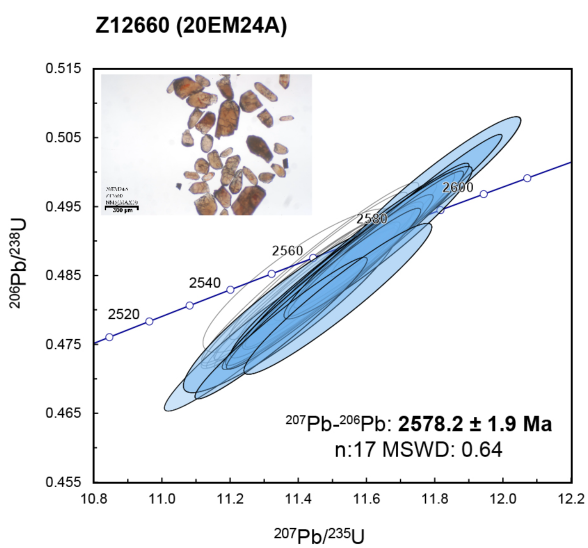

Figure 20: (a) Concordia diagram showing U-Pb SHRIMP results; light blue ellipses indicate the analyses used for the age calculation. Error ellipses are at 95% confidence level. Inset: Plain light photomicrograph of zircon mounted for SHRIMP analysis.

20EM24A: U-Pb results and interpretation

A total of 29 analyses were completed on 24 grains. Uranium contents vary from 269 to 771 ppm with Th/U ratios of 0.26-0.65. A single age population is defined with a weighted mean $^{207}Pb/^{206}Pb$ age of 2578.2 ± 1.9 Ma (n: 17, MSWD = 0.64, Fig. 20). Analyses younger than ca. 2575 Ma were not reproducible and therefore excluded from the age calculation (potentially affected by Pb-loss). The age is interpreted as the crystallization age of the monzogabbro.

10. Sample 20EM24B

Sample *20EM24B* is a pink, medium-grained, magnetic, foliated, hornblende quartz monzodiorite (Fig. 21). It contains xenoliths of monzogabbro (*20EM24A*) and is crosscut by monzogranite (*20EM24C*).

Figure 21: (a) Field photograph of the hornblende quartz monzodiorite (*20EM24B,* white arrow) and xenoliths of monzogabbro (*20EM24A*). (b) Photograph of the sample processed for U-Pb geochronology. Courtesy of Edith Martel.

20EM24B: Zircon description

Zircon recovered from sample *20EM24B* are of moderate quality, subhedral, and elongated (Fig. 22a). Crystals range in size from 200 to 500 µm, are generally brown in color and highly fractured. CL images reveal two distinct zones: i) partially resorbed, cores characterized by oscillatory zoning (Fig. 22b, c) surrounded by ii) bright rims with complex zoning (oscillatory and in some cases sector zoning, Fig. 22b, c), and iii) thin (<5µm) dark homogeneous external rims (Fig. 22b, c). It is worth noting that grains are very different from the ones recovered in sample *20EM24A* and therefore are not derived from the monzogabbro.

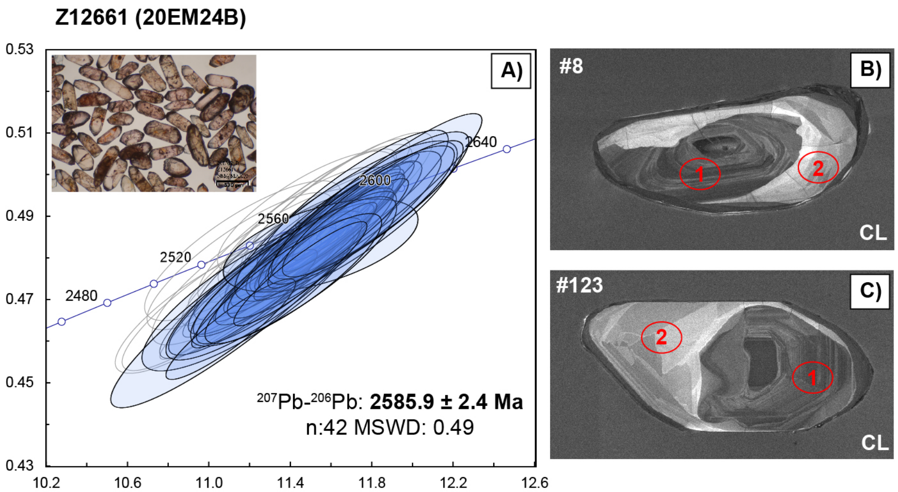

Figure 22: (a) Concordia diagram showing U-Pb SHRIMP results; light blue ellipses indicate the analyses used for the age calculation. Error ellipses are at 95% confidence level. Inset: Plain light photomicrograph of zircon mounted for SHRIMP analysis. (b, c) CL images of grains #8 and #123 and spot locations (red ellipses are ~20µm).

20EM24B: U-Pb results and interpretation

Sixty-six analyses on forty-two grains were performed on the darker cores and the bright rims, and range in age between 2601 and 2539 Ma. Uranium contents range from 31 to 682 ppm (Th/U between 0.19 and 0.93) and there is no correlation between uranium concentration and age. Several core and rim analyses overlap within error and are not reproducible suggesting that the scatter in the data is also the result of partial Pb-loss. Therefore, it is not possible to define two separate age populations. The oldest forty-two analyses of oscillatory-zoned cores (some of which are reproducible) yield a weighted mean $^{207}Pb/^{206}Pb$ age of 2585.9 ± 2.4 Ma (MSWD = 0.49, Fig. 22a). This population is interpreted as the best estimate for the crystallization of the monzodiorite. If this is correct, then the ca. 2578 Ma age of the monzogabbro xenoliths (*20EM24A*) must be interpreted as a minimum crystallization age.

11. <u>Sample 20EM24C</u>

Sample *20EM24C* is a white to pink, medium- to coarse-grained, hornblende-biotite monzogranite with rare feldspar megacrysts (Fig. 23). The monzogranite is commonly foliated to mylonitic with quartz ribbons defining the foliation. This sample crosscuts the quartz monzodiorite (*20EM24B*, Fig. 23) and contains xenoliths of the monzogabbro (*20EM24A*).

Figure 23: (a) Field photograph of the monzogranite (20EM24C; white arrow) intruding the quartz monzodiorite (20EM24B; top of image). (b) Photograph of the sample processed for U-Pb geochronology. Courtesy of Rebecca Canam.

20EM24C: Zircon description

Zircon grains recovered from this rock are of moderate quality. Grain morphology is dominated by well-faceted subequant to elongate prismatic crystals (Fig. 24a). The grains are clear to highly turbid and light brown to dark brown in colour. Many grains exhibit extensive metamictization and they range in size from 150 to 400 µm in the long dimension. In CL imaging the zircons display highly variable textures. Similar to sample *20EM24B*, a significant population preserves well-defined oscillatory zoning in the core which is in places recrystallized to a brighter zircon (Fig. 24b, c). All grains are characterized by a bright CL rim with faint oscillatory zoning (e.g., Fig 24b, c) that varies in thickness from 5 to 40 µm.

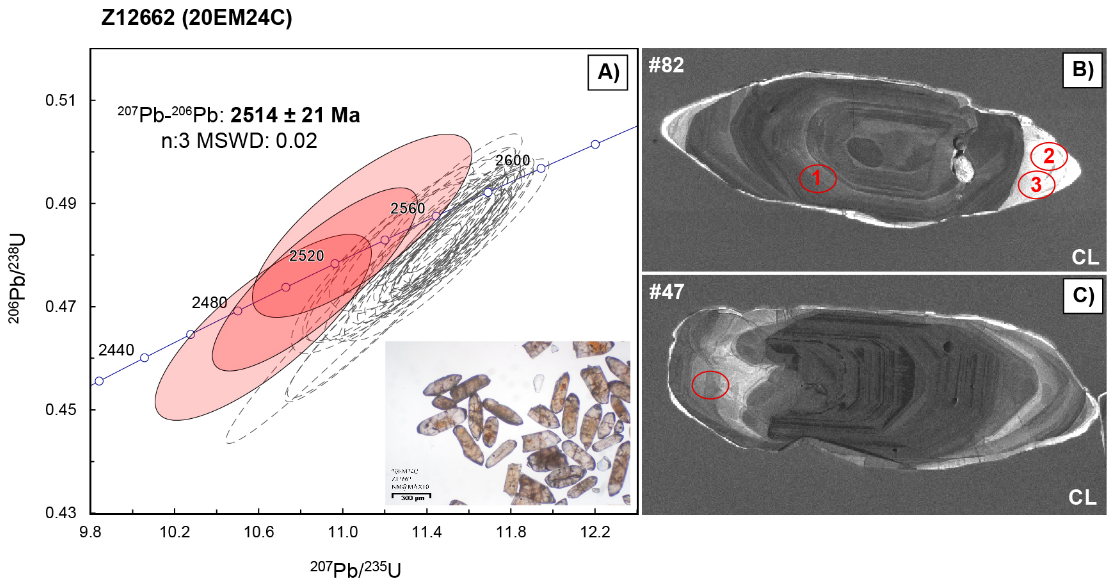

Figure 24: (a) Concordia diagram showing U-Pb SHRIMP results; red ellipses indicate the analyses used for the age calculation. Dashed grey ellipses are analyses on inherited grains. Error ellipses are at 95% confidence level. Inset: Plain light photomicrograph of zircon mounted for SHRIMP analysis. (b, c) CL image of grains #82 and #47 and spot locations (red ellipses are ~20µm).

20EM24C: U-Pb results and interpretation

Thirty-eight analyses were carried out on thirty grains. Analyses of the cores and internal rims (excluding the bright external ones) have U contents ranging between 53 and 286 ppm with Th/U ratios of 0.23-0.64. If taken together, these thirty-four analyses yield a weighted mean ^{207}Pb/^{206}Pb age of 2581.3 ± 2.5 Ma (MSWD = 1.09). The most external rims have low U (35-48 ppm) and low Th (ca. 1 ppm) concentrations. Three reproducible analyses (e.g., grain #82) on these rims yield a poorly defined weighted mean ^{207}Pb/^{206}Pb age of 2514 ± 21 Ma (Fig. 24a). Since field relationships show that sample *20EM24C* intrudes sample *20EM24B* and i) zircon morphology, ii) internal texture, iii) chemistry, and iv) age for cores and internal rims is comparable to the zircons in the monzodiorite, we interpret these grains as xenocrystic. The bright external rims with faint oscillatory zoning in sample *20EM24C* (e.g., grain #82) have not been observed in sample *20EM24B*. Therefore, we interpret the ca. 2514 Ma age as the best estimate for the crystallization age of the monzogranite.

12. <u>Sample 20EM28B</u>

Sample *20EM28B* is a fine- to medium-grained, foliated to mylonitic, non-magnetic monzogabbro (Fig. 25). The outcrop is highly altered with pervasive silicification and epidotization.

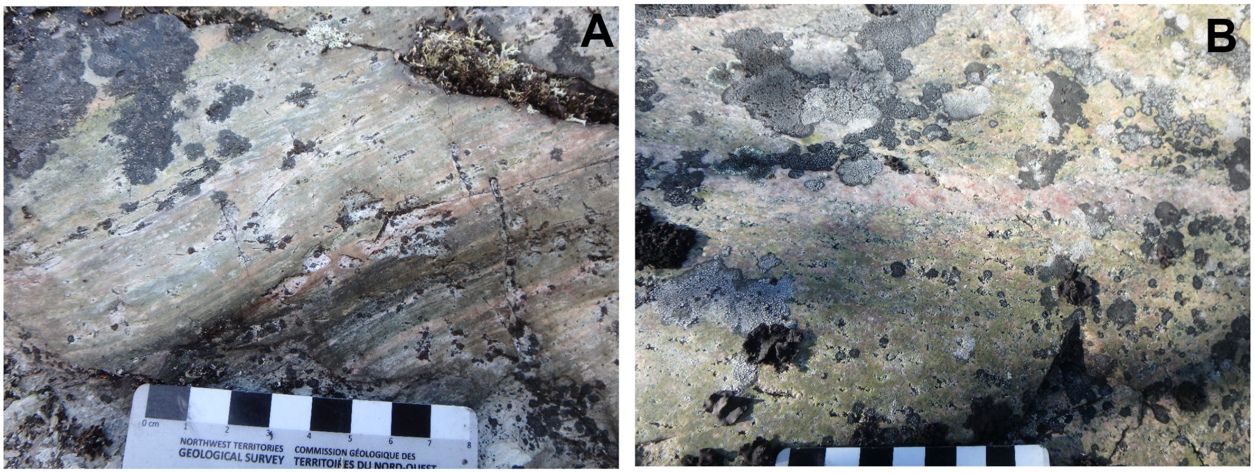

Figure 25: (a, b) Field photograph of sample *20EM28B*. The outcrop is highly altered with pervasive silicification and epidotization. Courtesy of Rebecca Canam.

20EM28B: Zircon description

Zircon recovered from sample *20EM28B* are of moderate quality, subhedral, and elongated (Fig. 26a). Crystals are small and range in size from 50 to 200 µm, are generally brown in colour with some iron staining and highly fractured. CL images reveal two distinct zones: partially resorbed bright cores characterized by oscillatory zoning surrounded by dark rims (Fig. 26b, c).

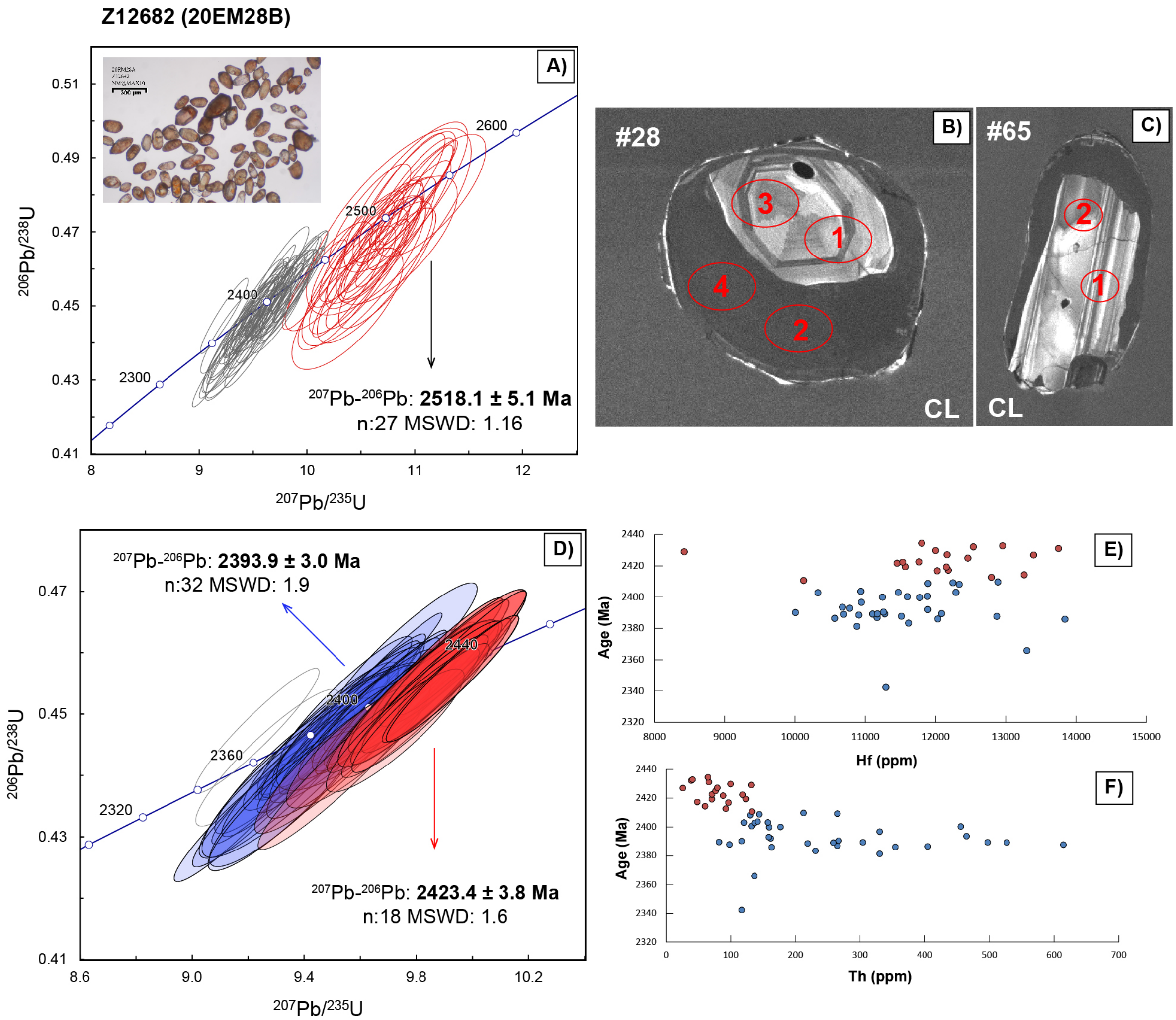

Figure 26: (a) Concordia diagram showing U-Pb SHRIMP results; red ellipses indicate the analyses used for the crystallization age calculation. Error ellipses are at 95% confidence level. Inset: Plain light photomicrograph of zircon mounted for SHRIMP analysis. (b, c) CL images of grains #28 and #65 and spot locations (red ellipses are ~20µm). (d) Concordia diagram showing U-Pb SHRIMP results for the two metamorphic rim age populations; grey ellipses have been excluded from the calculation; Error ellipses are at 95% confidence level. (e) Age (Ma) vs Hf (ppm) for the two rim populations; colors as in Fig. 26d. (f) Age (Ma) vs Th (ppm) for the two rim populations; colors as in Fig. 26d.

20EM28B: U-Pb results and interpretation

Eighty-two analyses were carried out on fifty-two grains targeting both the cores and the rims. Twenty-seven analyses of oscillatory-zoned cores yield a weighted mean $^{207}Pb/^{206}Pb$ age of 2518.1 ± 5.1 Ma (MSWD = 1.16, Fig. 26a). Cores are characterized by variable Th/U (0.2–1.0) and low Hf/Yb (20–70). Although CL images only show one dark rim, it is possible to identify two distinct domains based on their chemistry. The first one, characterized by low Th (30-130 ppm, Th/U: 0.05-0.46, Fig. 26f) and high Hf (11500-13750 ppm, Hf/Yb: 50-120, Fig. 26e) yield a weighted mean $^{207}Pb/^{206}Pb$ age of 2423.4 ± 3.8 Ma (n: 18, MSWD = 1.6, Fig. Fig. 26d). The second domain has higher Th contents (98-614 ppm, Fig. 26f) and generally lower Hf (10006-

13841 ppm, Fig. 26e). Thirty-two analyses of this domain return a weighted mean $^{207}Pb/^{206}Pb$ age of 2393.9 ± 3.0 Ma (MSWD = 1.9, Fig. 26d). The two youngest analyses were excluded from the calculation assuming minor Pb-loss. The core age is interpreted as the crystallization age of sample *20EM28B* while the younger rim ages, based on chemistry and textures, are interpreted to reflect multiple Siderian metamorphic recrystallization stages (i.e. Arrowsmith event).

13. Sample 20EM65A

This sample is located in the magnetic high southeast of the Nonacho basin (Fig. 2). Sample *20EM65A* is a dark greenish-grey, medium- to coarse-grained, strongly foliated, biotite-hornblende monzonite (Fig. 27). The monzonite is intruded by medium- to coarse-grained leucogranite.

Figure 27: (a) Field photograph of the biotite-hornblende monzonite (20EM65A). (b) Photograph of the sample processed for U-Pb geochronology. Courtesy of Rebecca Canam.

20EM65A: Zircon description

Zircon crystals recovered from sample *20EM65A* are turbid and dark brown in color stubby prisms, with few inclusions and fractions (Fig. 28a). A subset is clearer and colourless. Grain size ranges from 100 to 350 µm. CL imaging reveals that grains contain anhedral embayed cores with oscillatory zoning of varying brightness (Fig. 28b, c). Chemically homogeneous (flat CL character) subhedral to anhedral overgrowths surround the oscillatory-zoned cores (Fig. 28b, c).

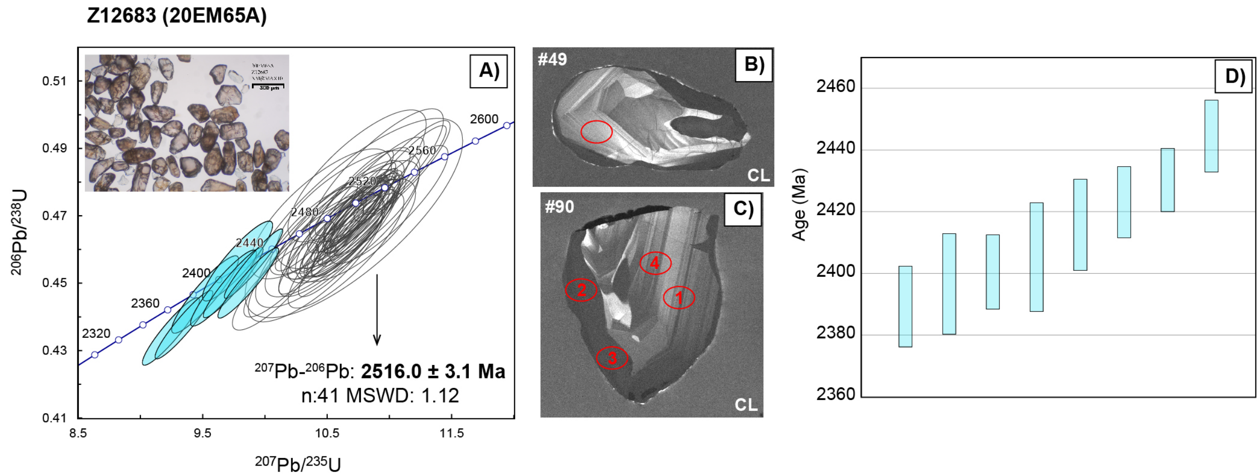

Figure 28: a) Concordia diagram showing U-Pb SHRIMP results; black ellipses indicate the analyses used for the crystallization age calculation. Light blue ellipses are analyses performed on rims. Error ellipses are at 95% confidence level. Inset: Plain light photomicrograph of zircon mounted for SHRIMP analysis. (b, c) CL images of grains #49 and #90 and spot locations (red ellipses are ~20µm). (d) Weighted average age plot of rim analyses not defining a single age population; error bars are at 95% confidence level.

20EM65A: U-Pb results and interpretation

Fifty-seven analyses were made on forty-three grains targeting the oscillatory-zoned grain interiors as well as the dark grain margins. The oldest forty-one analyses of grain interiors (gray ellipses in Fig. 28a) define a concordant cluster with a weighted mean ^{207}Pb/^{206}Pb age of 2516.0 ± 3.1 Ma (MSWD = 1.12), which is interpreted as the crystallization age of the monzonite. Zircon cores are characterized by U contents ranging between 0.5 and 2.04 (consistent with crystallization in a mafic magma) and relatively low Hf/Yb (14-87). Eight analyses of the darker zones have higher Hf/Yb (101-257) and lower Th/U ratios (0.11-0.24) and ages ranging between 2445 and 2389 Ma. These zones are interpreted to represent recrystallized areas of the older zircon. The analyses do not define a coherent age population (Fig. 28d) and the timing of the recrystallization is undetermined. However, these dates are consistent with the metamorphic age populations recognized in sample *20EM28B*.

14. <u>Sample 20EM66B</u>

This sample is located at an outcrop approximately 500 m north of *20EM65A* (Fig. 2). Sample *20EM66B* is a pinkish-grey, medium-grained, quartzofeldspathic orthogneiss (Fig. 29). The gneissic banding is defined by 1-5 cm-thick leucosome bands and the orthogneiss is crosscut by a red, amygdaloidal, porphyritic dyke.

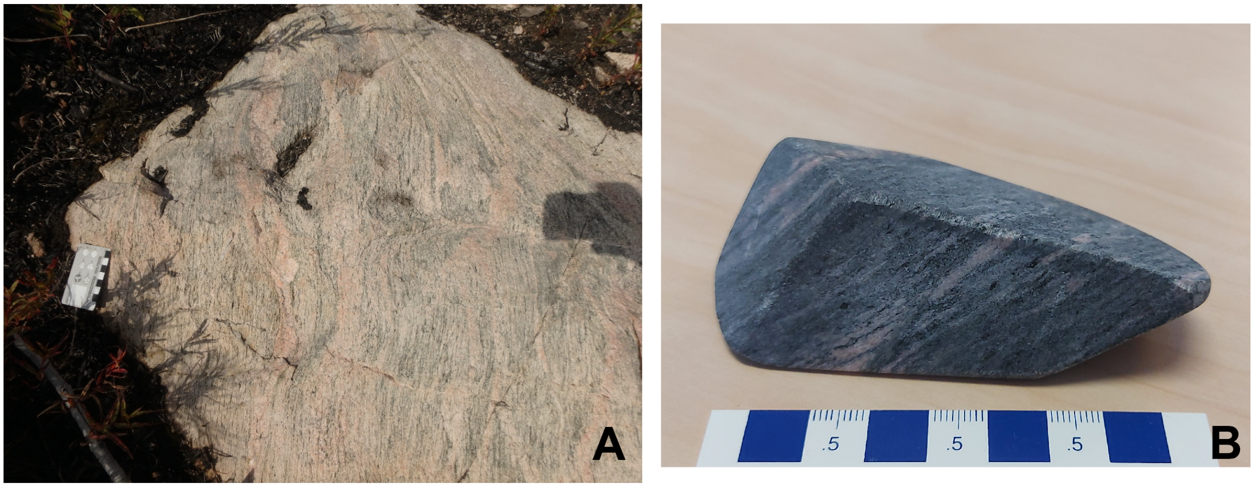

Figure 29: (a) Field photograph of the quartzofeldspathic orthogneiss (20EM66B). Care was taken to avoid the younger leucosome (light pink) components during sampling. (b) Photograph of the sample processed for U-Pb geochronology. Courtesy of Rebecca Canam.

20EM66B: Zircon description

Zircon recovered from sample *20EM66B* are of moderate quality, subhedral and elongated (Fig. 30a). Crystals range in size from 100 to 250 µm, are generally light brown in color and highly fractured. CL images reveal crystals with oscillatory zoning of varying brightness (Fig. 30b). No rims were observed.

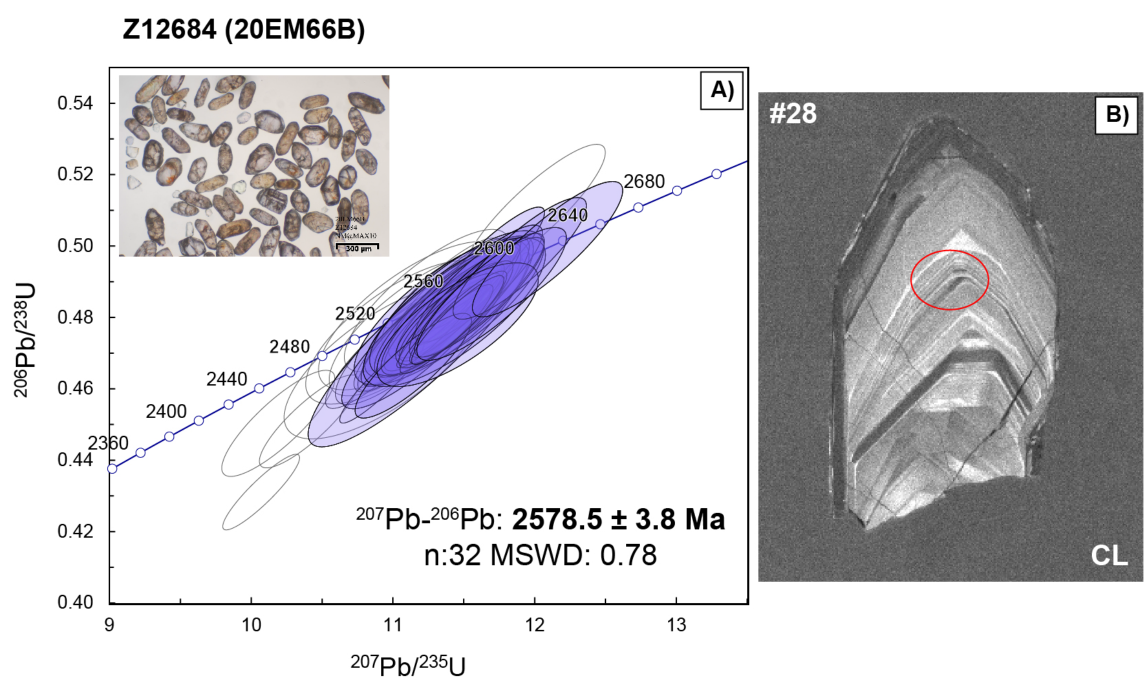

Figure 30: (a) Concordia diagram showing U-Pb SHRIMP results; purple ellipses indicate the analyses used for the age calculation. Error ellipses are at 95% confidence level. Inset: Plain light photomicrograph of zircon mounted for SHRIMP analysis. (b) CL image of grain #28 and spot location (red ellipses are ~20µm).

20EM66B: U-Pb results and interpretation

Forty-nine analyses on thirty-three oscillatory-zoned zircon crystals yield dates ranging from 2612 to 2499 Ma. The oldest thirty-two analyses yield a weighted mean $^{207}Pb/^{206}Pb$ age of 2578.5 ± 3.8 Ma (MSWD = 0.78, Fig. 30a). Ages younger than ca. 2565 Ma are not reproducible (e.g., grains #81, #67) – we interpret the scatter of the data as the result of partial Pb-loss. We interpret the ca. 2579 Ma age as the best estimate for the crystallization of the orthogneiss.

15. <u>Sample 20EM70A</u>

This sample is located approximately 1 km west of sample *20EM66B* (Fig. 2). Sample *20EM70A* is a pink, medium-grained, strongly foliated, magnetic, biotite-hornblende monzogranite (Fig. 31). This sample is crosscut by pink, coarse-grained to pegmatitic granitic dykes.

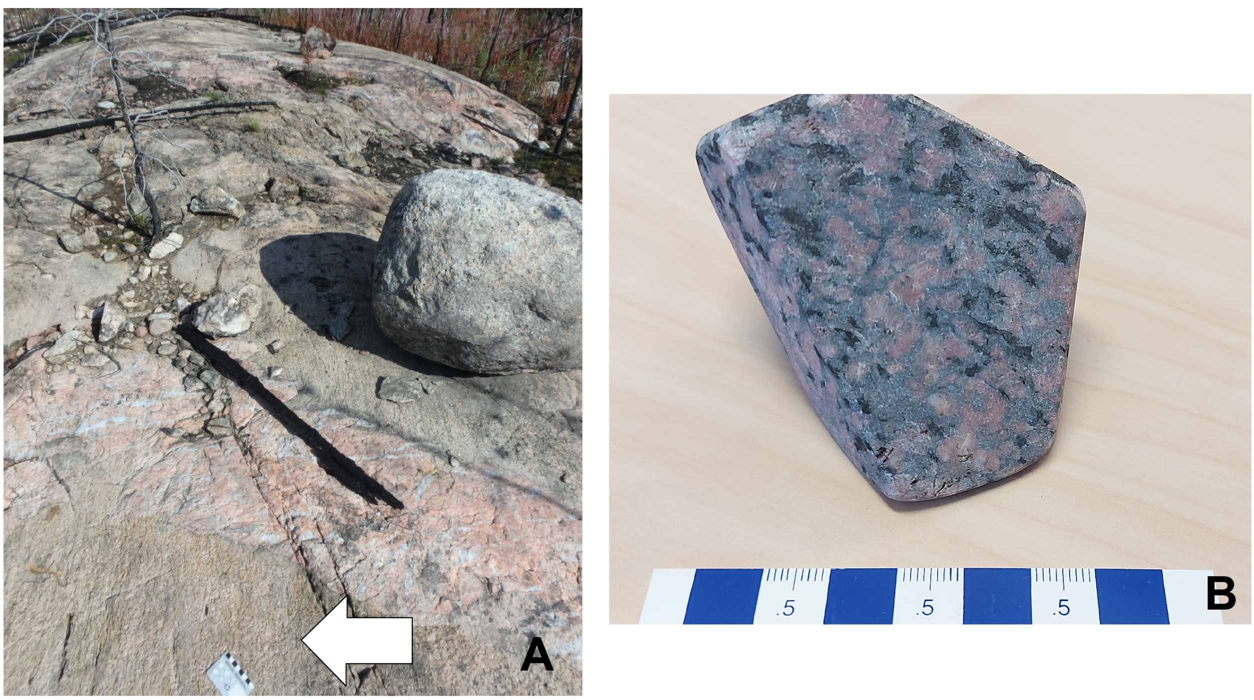

Figure 31: (a) Field photograph of the monzogranite (20EM70A; white arrow) crosscut by a coarse-grained granitic vein. (b) Photograph of the sample processed for U-Pb geochronology. Courtesy of Rebecca Canam.

20EM70A: Zircon description

Zircon grains occur as colourless clear to light brown euhedral to subhedral prisms (Fig. 32a). Some grains have sharp well terminated faces, whereas others show irregular surfaces indicative of resorption. Grain size varies from 100 to 300 µm. In CL, zircon typically shows partially resorbed oscillatory-zoned cores with variable brightness overgrown by darker domains with oscillatory zoning (Fig. 32b, c). Some grains exhibit a darker outer homogeneous rim.

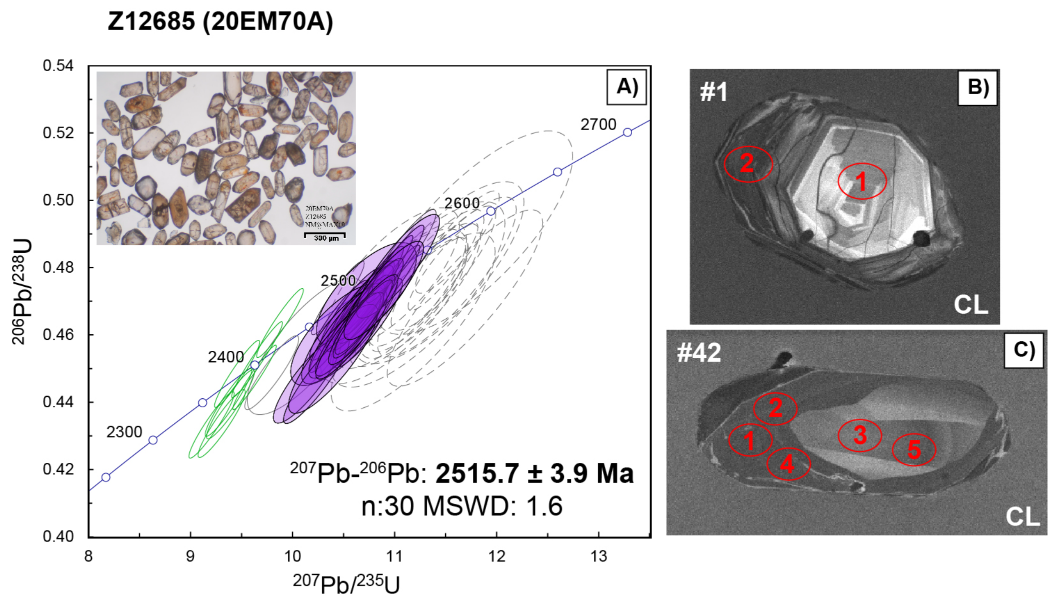

Figure 32: (a) Concordia diagram showing U-Pb SHRIMP results; purple ellipses indicate the analyses used for the crystallization age calculation. Dashed grey ellipses represent analyses on inherited grains. Green ellipses indicate analyses reflecting metamorphic recrystallization. Error ellipses are at 95% confidence level. Inset: Plain light photomicrograph of zircon mounted for SHRIMP analysis. (b, c) CL images of grains #1 and #42 and spot locations (red ellipses are ~20µm).

20EM70A: U-Pb results and interpretation

We carried out fifty-seven analyses on thirty-five individual zircon grains that yielded ages between 2653 Ma and 2379 Ma (Fig. 32a). The age data define three groups. Ages older than 2559 Ma (n: 15) have U contents of 35-300 ppm and are documented consistently from the innermost oscillatory-zoned parts of grains (e.g., analysis #1.1, Fig. 32b). The largest population corresponds to darker oscillatory-zoned portions of zircon crystals overgrowing the bright cores (e.g., analysis #1.2, Fig. 32b); these zones are characterized by higher U contents (120-713 ppm). Thirty analyses from this domain yield a weighted mean ^{207}Pb/^{206}Pb age of 2515.7 ± 3.9 Ma (MSWD = 1.6, Fig. 32a). The results from eight unzoned rims do not form a single age population and range in age between 2414 and 2379 Ma. Based on similar i) morphology, ii) internal CL textures and iii) chemistry we suggest the analyzed zircon cores are inherited from the orthogneiss host rock (i.e., sample *20EM66B*). We interpret the ca. 2516 Ma age as the best estimate for the crystallization age of the monzogranite. The remaining analyses are interpreted to reflect metamorphic recrystallization and are consistent with the metamorphic ages obtained for samples *20EM28B* and *20EM65A*.

Acknowledgments

The authors wish to thank Henry Brouwers from Great Slave Helicopters for the helicopter support in the field. We thank Nicole Rayner, Tom Pestaj, and Matthew Polivchuk for their help at the SHRIMP and SEM, and Sally Pehrsson for many fruitful discussions. The manuscript was improved through a critical review of Jeremy Powell.

References:

Aspler, L., 1985. Geology of the Nonacho Basin (Early Proterozoic) NWT (Unpublished Ph.D. thesis). Carleton University, Ottawa, ON.

Berman, R.G., Bostock, H., 1997. Metamorphism in the Northern Taltson Magmatic Zone, Northwest Territories. The Canadian Mineralogist 35, 1069–1091.

Berman, R.G., Pehrsson, S., Davis, W.J., Ryan, J.J., Qui, H., Ashton, K.E., 2013. The Arrowsmith orogeny: Geochronological and thermobarometric constraints on its extent and tectonic setting in the Rae craton, with implications for pre-Nuna supercontinent reconstruction. Precambrian Research 232, 44–69. https://doi.org/10.1016/j.precamres.2012.10.015

Bostock, H.H., 2014. The tectonic evolution of the Taltson Magmatic Zone: a reconnaissance study; Geological Survey of Canada, Open File 7683. doi:10.4095/295537

Bostock, H.H., Loveridge, W.D., 1988. Geochronology of the Taltson magmatic zone and its eastern cratonic margin, District of Mackenzie (Radiogenic Age and Isotopic Studies No. 2), Paper 88-2. Geological Survey of Canada.

Bostock, H.H., van Breemen, O., 1992. The timing of emplacement, and distribution of the Sparrow diabase dyke swarm, District of Mackenzie, Northwest Territories (Radiogenic Age and Isotopic Studies No. 6), Paper 92-2. Geological Survey of Canada.

Burwash, R.A., Baadsgaard, H., 1962. Yellowknife, Nonacho Age and Structural Relations, in: Stevenson, J.S. (Ed.), The Tectonics of the Canadian Shield. University of Toronto Press, pp. 22–29. https://doi.org/10.3138/9781487574161-006

Corrigan, D., Pehrsson, S., Wodicka, N., de Kemp, E., 2009. The Palaeoproterozoic Trans-Hudson Orogen: a prototype of modern accretionary processes. Geological Society, London, Special Publications 327, 457–479. https://doi.org/10.1144/SP327.19

Davis, W.J., Pehrsson, S.J., and Percival, J.A. 2015. Results of a U-Pb zircon geochronology transect across the southern Rae craton, Northwest Territories, Canada.; Geological Survey of Canada, Open File 7655, 1 .zip file. doi:10.4095/295610.

Henderson, J.F., 1939. Nonacho Lake, District of Mackenzie, Northwest Territories. Map 526A.

Ielpi, A., Martel, E., Fischer, B., Pehrsson, S.J., Tullio, M., Neil, B.J.C., 2021. A reappraisal of the Nonacho Basin (Northwest Territories, Canada): Record of post-orogenic collapse and marine flooding in the Palaeoproterozoic of the Rae Craton. Precambrian Research 358, 106140. https://doi.org/10.1016/j.precamres.2021.106140

Lowdon, J.A., Stockwell, C.H., Tipper, H.W., Wanless, R.K., 1963. Isotopic Ages (No. Paper 62-17), Age Determinations and Geological Studies. Geological Survey of Canada.

Ludwig, K.R., 2009. Isoplot 4.1, A geochronological toolkit for Microsoft Excel. Berkeley Geochronology Center Special Publication 4, p.76.

Martel, E., Canam, R., Neil, B.J.C., Landry, K., Terekova, A., Roy-Garand, A., Lockie, J., 2022. Preliminary geology of the basement rocks in the Nonacho Lake map sheet (NTS 75F), South Rae Craton, NWT, in preparation.

Martel, E., Pehrsson, S.J., Regis, D., Thiessen, E., Jamieson, D., Percival, J., Pierce, K.L., Acosta-Gongora, P., 2020. Geology of the McCann Lake area, South Rae craton, Northwest Territories (NTS 75G). NWT Open File 2020-02.

McGlynn, J.C., 1966. Thekulthili Lake area (No. Paper 66-1), Report of Activities. Geological Survey of Canada.

Schultz, M.E.J., Chacko, T., Heaman, L.M., Sandeman, H.A., Simonetti, A., Creaser, R.A., 2007. Queen Maud block: A newly recognized Paleoproterozoic (2.4–2.5 Ga) terrane in northwest Laurentia. Geology 35, 707–710. https://doi.org/10.1130/G23629A.1

Stern, R.A., 1997. The GSC Sensitive High Resolution Ion Microprobe (SHRIMP): Analytical Techniques of Zircon U–Th–Pb Age Determinations and Performance Evaluation. Radiogenic Age and Isotopic Studies, Report 10. Geological Survey of Canada, Current Research 1997-F, pp. 1–31.

Stern, R.A., Amelin, Y., 2003. Assessment of errors in SIMS zircon U–Pb geochronology using a natural zircon standard and NIST SRM 610 glass. Chem. Geol. 197, 111–146.

Taylor, F.C., 1971. Geology: Nonacho Lake, District of Mackenzie. Map 1281A.

van Breemen, O., Kjarsgaard, B.A., Tella, S., Lemkow, D., Aspler, L., 2013. U-Pb detrital zircon geochronology of clastic sedimentary rocks of the Paleoproterozoic Nonacho and East Arm basins, Thaidene Nene MERA study area, Chapter 4 (Open File No. 7196), Mineral and Energy Resource Assessment for the Proposed Thaidene Nene National Park Reserve in the Area of the East Arm of Great Slave Lake, Northwest Territories. Geological Survey of Canada.

Wanless, R.K., Stevens, R.D., Lachance, G.R., Edmonds, C.M., 1968. K-Ar Isotopic Ages, Report 8 (No. Paper 67-2), Age Determinations and Geological Studies. Geological Survey of Canada.